ChemPubSoc Europe

DOI: 10.1002/chem.201500877

CHEMISTRY A European Journal Full Paper

Imaging Agents

Synthesis and Characterization of Far-Red/NIR-Fluorescent BODIPY Dyes, Solid-State Fluorescence, and Application as Fluorescent Tags Attached to Carbon Nano-Onions**

Juergen Bartelmess,[a] Michele Baldrighi,[a] Valentina Nardone,[b, c] Emilio Parisini,[b] David Buck,[d] Luis Echegoyen,[d] and Silvia Giordani*[a]

Abstract: A series of π-extended distyryl-substituted boron dipyrromethene (BODIPY) derivatives with intense far-red/near-infrared (NIR) fluorescence was synthesized and characterized, with a view to enhance the dye's performance for fluorescence labeling. An enhanced brightness was achieved by the introduction of two methyl substituents in the *meso* positions on the phenyl group of the BODIPY molecule; these substituents resulted in increased structural rigidity. Solid-state fluorescence was observed for one of the distyryl-substituted BODIPY derivatives. The introduction of a terminal bromo substituent allows for the subsequent immobilization of the BODIPY fluorophore on the surface of carbon nano-onions (CNOs), which leads to potential imaging agents for biological and biomedical applications. The far-red/NIR-fluorescent CNO nanoparticles were characterized by absorption, fluorescence, and Raman spectroscopies, as well as by thermogravimetric analysis, dynamic light scattering, high-resolution transmission electron microscopy, and confocal microscopy.

Introduction

Boron dipyrromethenes (BODIPYs) are versatile dyes that have been applied as fluorescence indicators,[1] as chromophores in dye-sensitized solar cells,[2] as triplet photosensitizers,[3,4] and, based on their ability to induce the formation of singlet oxygen upon illumination, in the photodynamic therapy of cancer.[5] The major advantage of BODIPY dyes is their synthetic versatility in combination with their high photostability.[6–8] For biological applications, various BODIPY fluorophores are commercially available as labels for a multitude of purposes.[9] A high fluorescence quantum yield is desirable for any application in imaging, because this allows for the detection of the fluorescence signal even at a very low fluorophore concentration and gives rise to bright images. One general approach for increasing the fluorescence quantum yield of fluorophores is to increase the rigidity of the dye's molecular structure. This concept was previously reported for BODIPY dyes and can be readily accomplished by hindering the rotation of substituents in the *meso* position of the BODIPY structure.[10–13] For *meso*-pyridyl-substituted BODIPYs, for example, the fluorescence quantum yield was increased from 0.30 to 0.98 by introducing two chloro substituents in the 3- and 5-positions of the pyridine moiety.[13]

Solid-state fluorescence is an interesting but rare characteristic of organic dyes in general and BODIPYs in particular. A variety of different synthetic strategies to achieve solid-state fluorescence have been investigated. Leading examples include the introduction of bulky substituents,[14–19] dimerization,[20,21] and control over the BODIPY aggregation pattern by introducing trifluoromethyl substituents.[22] All of these approaches modify the BODIPY molecular structure to suppress π–π stacking of the BODIPY building blocks in the solid state. This general concept has also been reported for other fluorophores.[23,24]

Carbon nanomaterials are widely employed as imaging agents in biology and biomedicine by using a variety of approaches.[25] However, the application of BODIPY fluorophores in combination with carbon nanostructures has not been widely explored. We recently reported our findings with carbon nano-onions (CNOs) labeled with a green-fluorescent

[a] Dr. J. Bartelmess, Dr. M. Baldrighi, Prof. Dr. S. Giordani
Istituto Italiano di Tecnologia (IIT)
Nano Carbon Materials
Via Morego 30, 16163 Genova (Italy)
E-mail: silvia.giordani@iit.it

[b] Dr. V. Nardone, Dr. E. Parisini
Istituto Italiano di Tecnologia (IIT)
Center for Nano Science and Technology
Via G. Pascoli 70/3, 20133 Milano (Italy)

[c] Dr. V. Nardone
Department of Chemistry
Material and Chemical Engineering
Politecnico di Milano
Piazza Leonardo Da Vinci, 20133 Milano (Italy)

[d] D. Buck, Prof. Dr. L. Echegoyen
Department of Chemistry
University of Texas at El Paso
500 W. University Ave., El Paso, TX 79968 (USA)

[**] NIR: Near infrared; BODIPY: boron dipyrromethene.

Supporting information for this article is available on the WWW under http://dx.doi.org/10.1002/chem.201500877.

BODIPY dye for high-resolution cellular imaging of MCF-7 human breast cancer cells.[26] The CNOs act as molecular shuttles and facilitate the delivery of the dye molecules into the cells. CNOs are an exciting class of carbon nanomaterials,[27] which are typically prepared by thermal annealing of nanodiamonds[28–30] and various other methods.[31] In the past, CNOs were employed in a variety of fields and their synthetic surface modification was investigated.[32,33] In addition to biomedical imaging, other prominent examples for which CNOs have been successfully employed include tribology,[34,35] energy applications like lithium-ion batteries[36,37] and fuel cells,[38] catalysis,[39,40] and electronic applications, such as terahertz shielding[41] and in capacitors.[42,43] The low cytotoxicity observed for our functionalized CNOs[44,45] is one important aspect that renders the CNOs as ideal vectors for biological and biomedicinal applications.

In the present study, we prepared novel, highly fluorescent BODIPY dyes that emit in the biomedically important far-red/near-infrared (NIR) region and we investigated their intrinsic properties and combined them with carbon nano-onions, which led to a far-red/NIR-fluorescent nanoprobe. In addition, this report highlights the single-crystal solid-state fluorescence features of one of the BODIPY derivatives, a property that is of special interest for future applications in optical devices.

Results and Discussion

The synthetic procedures are summarized in Scheme 1 and Scheme 2. Briefly, the initial BODIPY fluorophore **1** was prepared by a one-pot, multistep reaction in satisfactory yield by

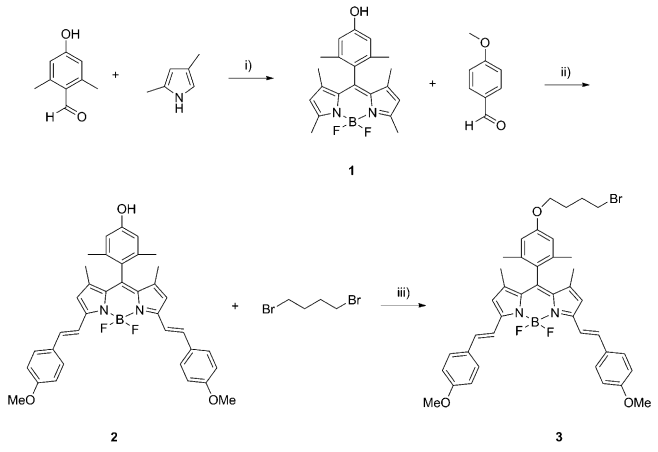

Scheme 1. Synthesis of BODIPY derivatives **1**, **2**, and **3**. i) 1. Dichloromethane/ethanol, trifluoroacetic acid, N_2; 2. tetrachloro-1,4-benzoquinone (chloranil); 3. dichloromethane, *N*,*N*-diisopropylethylamine; 4. boron trifluoride etherate; ii) toluene, piperidine, glacial acetic acid, $Mg(ClO_4)_2$, Dean–Stark condenser; iii) acetone, K_2CO_3.

using ethanol as a cosolvent with dichloromethane, as previously described.[13] BODIPY **1** was synthesized earlier by another method;[46] however, the synthetic strategy presented herein led to a significant increase of the yield from 21 to 47%. A Knoevenagel type condensation was subsequently performed,

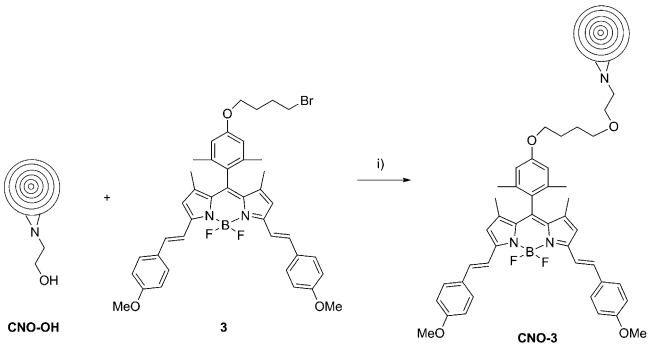

Scheme 2. Functionalization of hydroxy-terminated **CNO-OH** with BODIPY **3**. i) Acetone, K_2CO_3.

by following reported reaction conditions.[47] The reaction with *p*-anisaldehyde led to the dark-blue, red-fluorescent BODIPY derivative **2**. Recrystallization from a dichloromethane solution, layered with methanol, resulted in the formation of X-ray-quality crystals. From **2**, an excess of 1,4-dibromobutane, in the presence of K_2CO_3 as a base, was used to prepare the bromo-terminated BODIPY alkyl ether derivative **3**. X-ray-quality crystals were obtained by recrystallization of **3** from a hexane-layered dichloromethane solution. Toward the functionalization of CNOs, another etherification was conducted with the previously reported **CNO-OH**[48] and BODIPY **3. CNO-OH** was dispersed in acetone and heated under reflux together with BODIPY derivative **3** in the presence of K_2CO_3. The functionalized CNOs were recovered by filtration with a nylon membrane (0.2 μm) and purified by careful washing with plenty of solvent, until all non-CNO-bound fluorophore and other impurities were removed.

Spectroscopic analysis of the BODIPY dyes revealed an intense green fluorescence for **1** and red/NIR fluorescence for **2** and **3**, with high fluorescence quantum yields. The absorption and fluorescence features are typical for the substitution pattern of the BODIPY derivatives; see Figure 1 and Table 1. Com-

Table 1. Photophysical data for **1**, **2**, and **3** in chloroform and DMSO.[a]

Compound	Solvent	λ_{Abs} max [nm]	$\varepsilon \times 10^3$ [$M^{-1}cm^{-1}$]	Φ_F	λ_{Em} max [nm]
1	chloroform[b]	504	80.7	0.94	517
2	chloroform[b]	644	94.0	0.83	664
2	DMSO[c]	648	117.8	0.82	670
3	chloroform[c]	644	125.8	0.82	662
3	DMSO[c]	649	130.9	0.82	669

[a] λ_{Abs} max: absorption maximum; ε: molar extinction coefficient; Φ_F: fluorescence quantum yield; λ_{Em} max: emission maximum. [b] Measured relative to *meso*-phenol-substituted BODIPY. Quantum yield: 0.64 in toluene.[49] [c] Measured relative to zinc(II)tetra-*tert*-butylphthalocyanine. Quantum yield: 0.27 in THF.[50]

pound **1** has an absorption maximum at 504 nm, an emission maximum at 517 nm, and a fluorescence quantum yield of 0.94 (in chloroform). Distyryl-substituted BODIPY derivatives **2** and **3** show absorption maxima in chloroform at 644 nm and

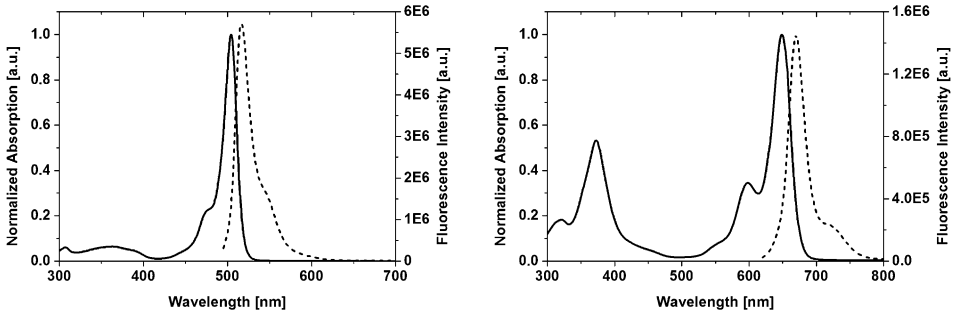

Figure 1. Absorption (solid line) and fluorescence (dotted line) spectra of **1** in chloroform (left) and **3** in DMSO (right).

emission maxima at 664 and 662 nm, respectively. The fluorescence quantum yields of **2** and **3** are about 0.82 in both chloroform and DMSO. The absorption and emission maxima in DMSO are slightly bathochromically shifted, by about 5 nm for the absorption and 7 nm for the emission for both compounds.

The molecular structures of **2** and **3** were investigated by means of X-ray crystallography. In the structures (Figure 2; see also Table S1 and Figure S1 in the Supporting Information), the boron atom is coordinated in a tetrahedral fashion by two nitrogen and two fluorine atoms. In both compounds, the BODIPY core is nearly planar, because the value of the dihedral angle between the two pyrrole rings is 7.97° for **2** and 2.62° for **3**. In both molecules, the *meso*-phenyl group is on a plane that is nearly orthogonal to the plane of the 12-membered cycle, with dihedral angles of −83.8(5)° for **3** and −82.8(2)° for **2**. This conformation limits the possible resonance between the indacene core and the phenyl substituent, as confirmed by the length of the C–C bond that links the two moieties (1.498 (3) in **2** and 1.492(6) Å in **3**), which indicates a single-bond character. In both molecules, extended conjugation is provided by the two styryl substituents linked to the indacene core. These lateral chains are also involved in the intermolecular stabilization of **2**, in which they form antiparallel arrangements involving π–π interactions between neighboring molecules. However, no such packing interactions are observed in the crystal lattice of **3**. The crystal packing of **2** and **3** is illustrated in Figure 3 and clearly reveals the presence of π–π stacking interactions in the case of **2** but not of **3**. The difference between BODIPY **2** and **3** in their crystal packing, that is, the absence of π–π stacking interactions between BODIPY molecules in **3**, results in the latter's intense solid-state fluorescence (Figure 4; see also Figure S2 in the Supporting Information). Confocal microscopy of the single crystals of **3** revealed an intense red-fluorescence signal, which was not observed for single crystals of **2**. The emission maximum of crystalline **3** is bathochromically shifted relative to that of **3** in solution and is located at 703 nm (Figure S2 in the Supporting Information). This finding was somehow unexpect-

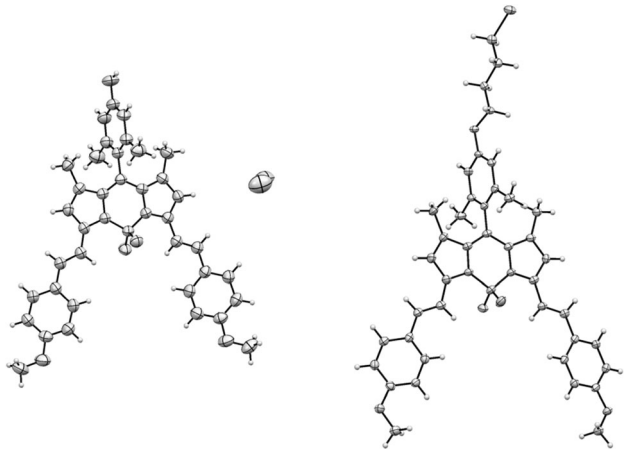

Figure 2. ORTEP representation of the molecular structures of **2** (left) and **3** (right).

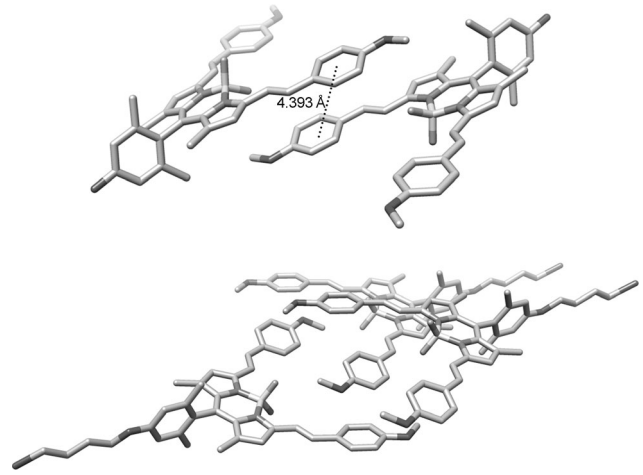

Figure 3. Crystal packing of **2** (top) and **3** (bottom).

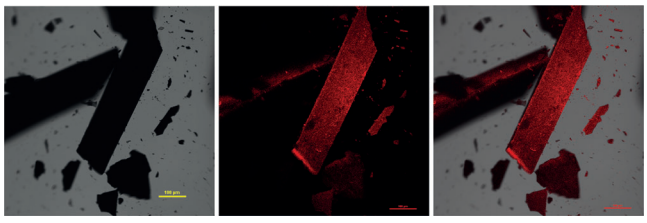

Figure 4. Laser confocal microscopy images of single crystals of BODIPY derivative **3**. Left: bright-field image. Center: Fluorescence of the BODIPY dye. Right: Overlay of the bright field and fluorescence images. Excitation at 560 nm; detection of the fluorescence in a range of (700±35) nm. Scale bar: 100 μm.

ed but is in line with the general observation of solid-state fluorescence in BODIPY fluorophores in which π–π stacking is impaired,[14–21] although BODIPY **3** lacks the bulky substituents of most reported solid-state fluorescers. The introduction of a relatively small, linear 1-bromobutane chain is sufficient to prevent π–π stacking in the crystal of **3**. These findings could lead to future designs of BODIPY derivatives with solid-state fluorescence features.

The prepared BODIPY-functionalized carbon nano-onions **CNO-3** were characterized by a multitude of methods. The results of the thermogravimetric analysis (TGA) of pristine CNOs and **CNO-OH** are consistent with previously reported results, with a weight loss of 10.7% at 500 °C observed for **CNO-OH** (Table 2 and Figure 5, left).[48] The TGA of BODIPY-tagged **CNO-3** revealed an additional weight loss of 9%, which is indicative of the successful attachment of the BODIPY fluorophores to the CNOs. For the degree of functionalization of the CNOs, based on the weight loss derived from the TGA analyses and by following a previously reported approach,[51] we estimate that about 12 BODIPY molecules are attached to each individual CNO. With the high molecular volume of the BODIPY molecule taken into account, we believe that this loading result is reasonable.

Table 2. Thermal analysis data of pristine CNOs, **CNO-OH**, and **CNO-3** derived from TGA.

Sample	Weight loss at 500 °C [%]	Decomposition temperature [°C]	Number of functional groups per CNO
pristine CNOs	1.5	701	–
CNO-OH	10.7	698	114
CNO-3	19.7	691	12

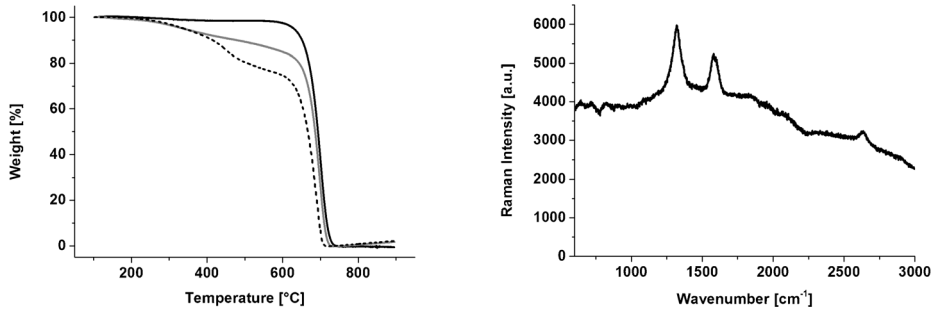

Figure 5. TGA (left) of pristine CNOs (black), **CNO-OH** (gray), and **CNO-3** (dotted). Raman spectrum of **CNO-3** (right).

The pristine CNOs and **CNO-OH** utilized in this study show similar Raman spectra to those already reported (see Figure S3 in the Supporting Information).[38] However, Raman spectroscopy of **CNO-3** revealed clear differences to the results observed for **CNO-OH**. The excitation wavelength of the Raman laser source was 632 nm, which is close to the absorption maximum of **3**, so an intense background fluorescence signal was observed due to the presence of the BODIPY dye (Figure 5, right). The fluorescence of **CNO-3** was further analyzed by steady-state fluorescence spectroscopy. Photoexcitation of a dispersion of **CNO-3** in DMSO at 615 nm revealed a BODIPY-centered emission with a maximum at about 660 nm. UV/Vis/NIR absorption measurements showed that, next to the typical broad plasmonic absorption of the CNOs, a BODIPY-centered absorption appears at around 650 nm (Figure 6, top). Due to the large CNO absorption, the fluorescence quantum yield of **CNO-3** is lower than the one observed for BODIPY derivative **3**. This effect was previously reported for other CNO–dye conjugates but did not significantly alter their excellent performance in biomedical imaging.[26,45] We estimated the fluorescence quantum yield of **CNO-3** to be about 0.5 by comparing the fluorescence intensities of **CNO-3** and BODIPY **3** at a comparable BODIPY-centered absorption at the excitation wavelength (Figure 6, bottom). This value is remarkably high in comparison with the fluorescence quantum yields of other dyes conjugated to different carbon nanomaterials.[25]

To probe the fluorescence of the far-red/NIR BODIPY-tagged **CNO-3** bulk material, laser confocal microscopy imaging was performed. The CNOs were dispersed in a drop of water on a polystyrene slide, which led to the deposition of CNO aggregates on the polymeric surface, then the sample was dried. In 3D *z*-stacking images, the red fluorescence was observed throughout the whole sample area (Figure 7; see also Figure S4 in the Supporting Information for the corresponding bright-field image). Additional confocal microscopy images supported this conclusion (see Figure S5 in the Supporting Information).

High-resolution TEM analysis of the pristine CNOs shows the quasispherical onion diameter ranges from 5 to 7 nm (Figure 8). The inner shell of the CNOs is close to 1 nm, which suggests that it consists of fewer than 100 carbon atoms.

Dynamic light scattering was carried out to determine the hydrodynamic radius of the dispersed CNOs. Dispersions of **CNO-OH** and **CNO-3** were prepared in a phosphate-buffered saline solution at pH 7.4 in order to mimic biological conditions. **CNO-OH** revealed a size distribution with a major component of the particle size of about 240 nm. The zeta (*Z*) potential of **CNO-OH** in a 0.01 M phosphate buffer was determined to be −27 mV. The average *Z* potential of **CNO-3** was found to be lower than that of **CNO-OH**, with typical average values of −15 mV. This is consistent with the introduction of the hydrophobic BODIPY molecule onto the **CNO-OH** surface, which leads to a reduction of the hydroxy functionalities on the CNO surface. The average hydrodynamic radius of **CNO-3** was found to be comparable to that of **CNO-OH**.

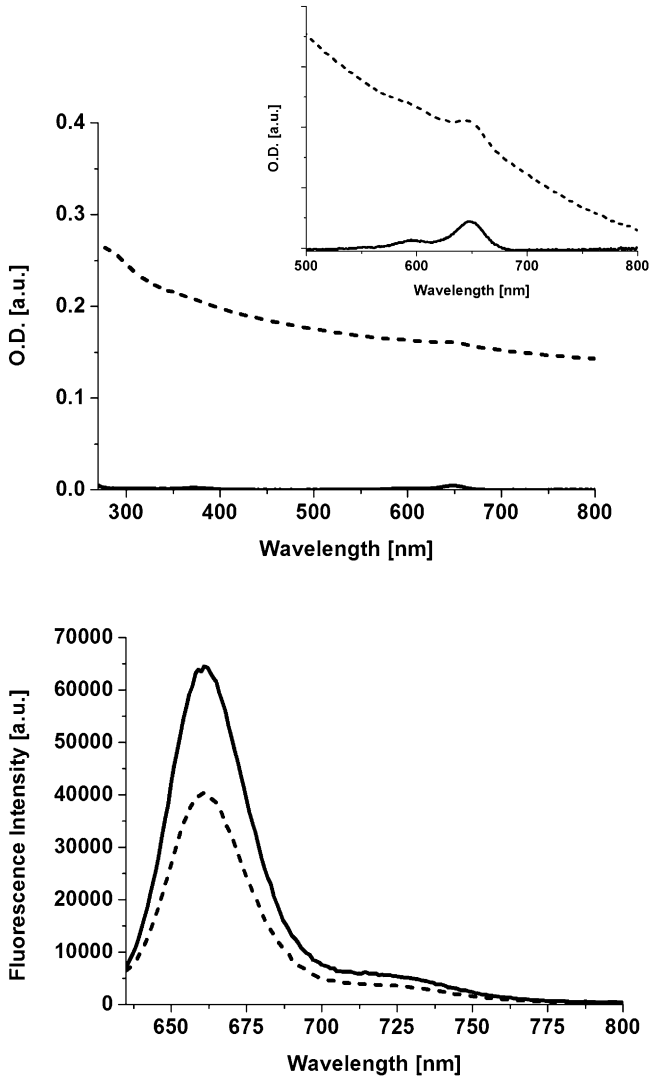

Figure 6. Absorption (top) and fluorescence (bottom) spectra for the comparison of BODIPY **3** (solid line) with **CNO-3** (dotted line). Both samples exhibit the same BODIPY-centered absorption at the excitation wavelength of 615 nm. Inset top: Magnified absorption spectra for comparison.

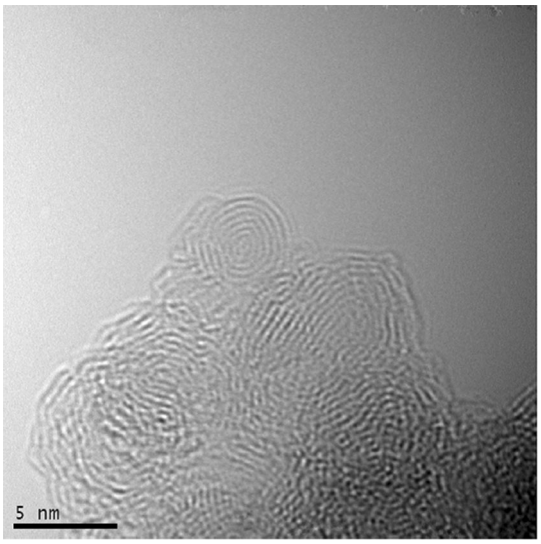

Figure 8. Representative high-resolution TEM image of the pristine CNO starting material.

Conclusion

We report the preparation and characterization of bright BODIPY fluorophores and their subsequent use for the decoration of OH-terminated CNOs, which led to far-red/NIR-fluorescent CNO nanoparticles. The fluorescence quantum yield of the BODIPY fluorophores was successfully increased to values as high as 0.94 for **1** and 0.83 for the far-red/NIR-fluorescent BODIPY derivatives. This was achieved by the introduction of methyl groups on the *meso*-phenol substituent of BODIPY, which results in increased rigidity of the BODIPY molecular structure. Of special interest is the solid-state fluorescence observed for single crystals of BODIPY derivative **3**. Absorption, fluorescence, and Raman spectroscopies, thermogravimetric analysis, and laser confocal microscopy of **CNO-3** revealed the successful functionalization and promising properties for future applications in biological and biomedical imaging. The far-red/NIR-fluorescent CNOs presented in this report will be the starting materials for the preparation of theranostic nanomaterials that combine imaging with drug delivery and targeting. This work is ongoing in our laboratories.

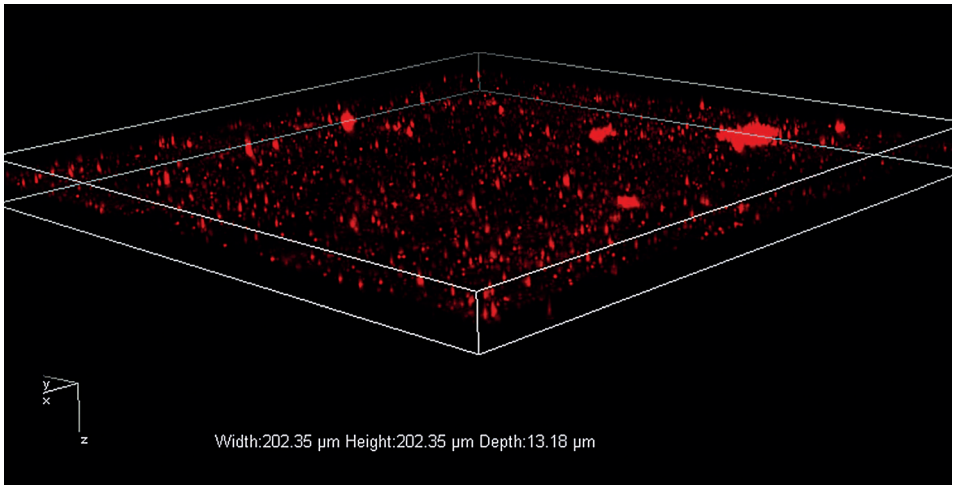

Figure 7. 3D Laser confocal microscopy *z*-stacking image of **CNO-3** aggregates deposited on polystyrene, which illustrates the intense red fluorescence of the BODIPY-functionalized CNOs. Excitation at 647 nm; detection of the fluorescence in a range of (700±35) nm. Scale as indicated.

Experimental Section

All synthetic procedures, instrumental details, and additional experimental procedures are summarized in the Supporting Information, along with additional figures. CCDC-1051088 (**2**) and 1051089 (**3**) contain the supple-

mentary crystallographic data for this paper. These data can be obtained free of charge from The Cambridge Crystallographic Data Centre via www.ccdc.cam.ac.uk/data_request/cif.

Acknowledgements

The authors wish to thank the Istituto Italiano di Tecnologia (IIT) for funding. We are grateful to Marco Scotto (IIT Nanophysics) for support with the laser confocal microscopy, Sine Mandrup Bertozzi (IIT D3) for HRMS measurements, and the D3 and Nanophysics Departments at IIT for instrumental support. E.P. thanks the European Union for financial support ("Marie Curie" FP7 IRG grant no. 268231). L.E. wishes to thank the NSF PREM Program (DMR-1205302) and the Robert A. Welch Foundation (grant AH-0033) for generous financial support.

Keywords: carbon · nanostructures · fluorescent probes · imaging agents · solid-state fluorescence

[1] N. Boens, V. Leen, W. Dehaen, *Chem. Soc. Rev.* **2012**, *41*, 1130.
[2] S. P. Singh, T. Gayathri, *Eur. J. Org. Chem.* **2014**, 4689.
[3] J. Zhao, W. Wu, J. Sun, S. Guo, *Chem. Soc. Rev.* **2013**, *42*, 5323.
[4] J. Bartelmess, A. J. Francis, K. A. El Roz, F. N. Castellano, W. W. Weare, R. D. Sommer, *Inorg. Chem.* **2014**, *53*, 4527.
[5] A. Kamkaew, S. H. Lim, H. B. Lee, L. V. Kiew, L. Y. Chung, K. Burgess, *Chem. Soc. Rev.* **2013**, *42*, 77.
[6] A. Loudet, K. Burgess, *Chem. Rev.* **2007**, *107*, 4891.
[7] G. Ulrich, R. Ziessel, A. Harriman, *Angew. Chem. Int. Ed.* **2008**, *47*, 1184; *Angew. Chem.* **2008**, *120*, 1202.
[8] B. Hinkeldey, A. Schmitt, G. Jung, *ChemPhysChem* **2008**, *9*, 2019.
[9] *The Molecular Probes Handbook: A Guide to Fluorescent Probes and Labeling Technologies*, 10th ed. (Eds.: I. Johnson, M. T. Z. Spence), Life Technologies Corporation, Carlsbad (CA), **2010**.
[10] H. L. Kee, C. Kirmaier, L. Yu, P. Thamyongkit, W. J. Youngblood, M. E. Calder, L. Ramos, B. C. Noll, D. F. Bocian, W. R. Scheidt, R. R. Birge, J. S. Lindsey, D. Holten, *J. Phys. Chem. B* **2005**, *109*, 20433.
[11] Q. Zheng, G. Xu, P. N. Prasad, *Chem. Eur. J.* **2008**, *14*, 5812.
[12] H. Sunahara, Y. Urano, H. Kojima, T. Nagano, *J. Am. Chem. Soc.* **2007**, *129*, 5597.
[13] J. Bartelmess, W. W. Weare, N. Latortue, C. Duong, D. S. Jones, *New. J. Chem.* **2013**, *37*, 2663.
[14] D. Zhang, Y. Wen, Y. Xiao, G. Yu, Y. Liu, X. Qian, *Chem. Commun.* **2008**, 4777.
[15] T. Ozdemir, S. Atilgan, I. Kutuk, L. T. Yildirim, A. Tulek, M. Bayindir, E. U. Akkaya, *Org. Lett.* **2009**, *11*, 2105.
[16] T. T. Vu, S. Badré, C. Dumas-Verdes, J.-J. Vachon, C. Julien, P. Audebert, E. Y. Senotrusova, E. Y. Schmidt, B. A. Trofimov, R. B. Pansu, G. Clavier, R. Méallet-Renault, *J. Phys. Chem. C* **2009**, *113*, 11844.
[17] E. Y. Schmidt, B. A. Trofimov, A. I. Mikhaleva, N. V. Zorina, N. I. Protzuk, K. B. Petrushenko, I. A. Ushakov, M. Y. Dvorko, R. Méallet-Renault, G. Clavier, T. T. Vu, H. T. T. Tran, R. B. Pansu, *Chem. Eur. J.* **2009**, *15*, 5823.
[18] Y. Kubota, J. Uehara, K. Funabiki, M. Ebihara, M. Matsui, *Tetrahedron Lett.* **2010**, *51*, 6195.
[19] Y. Ooyama, Y. Hagiwara, Y. Oda, H. Fukuoka, J. Ohshita, *RSC Adv.* **2014**, *4*, 1163.
[20] H. Xi, C.-X. Yuan, Y.-X. Li, Y. Liu, X.-T. Tao, *CrystEngComm* **2012**, *14*, 2087.
[21] L. Gai, H. Lu, B. Zou, G. Lai, Z. Shen, Z. Li, *RSC Adv.* **2012**, *2*, 8840.
[22] S. Choi, J. Bouffard, Y. Kim, *Chem. Sci.* **2014**, *5*, 751.
[23] Y. Ooyama, T. Okamoto, T. Yamaguchi, T. Suzuki, A. Hayashi, K. Yoshida, *Chem. Eur. J.* **2006**, *12*, 7827.
[24] Y. Ooyama, Y. Kagawa, Y. Harima, *Eur. J. Org. Chem.* **2007**, *2007*, 3613.
[25] J. Bartelmess, S. J. Quinn, S. Giordani, *Chem. Soc. Rev.* **2015**, DOI: 10.1039/c4s00306c.
[26] J. Bartelmess, E. De Luca, A. Signorelli, M. Baldrighi, M. Becce, R. Brescia, V. Nardone, E. Parisini, L. Echegoyen, P. P. Pompa, S. Giordani, *Nanoscale* **2014**, *6*, 13761.
[27] D. Ugarte, *Nature* **1992**, *359*, 707.
[28] V. L. Kuznetsov, M. N. Aleksandrov, I. V. Zagoruiko, A. L. Chuvilin, E. M. Moroz, V. N. Kolomiichuk, *Carbon* **1991**, *29*, 665.
[29] V. L. Kuznetsov, A. L. Chuvilin, Y. V. Butenko, I. Y. Mal'kov, V. M. Titov, *Chem. Phys. Lett.* **1994**, *222*, 343.
[30] A. Palkar, F. Melin, C. M. Cardona, B. Elliott, A. K. Naskar, D. D. Edie, A. Kumbhar, L. Echegoyen, *Chem. Asian J.* **2007**, *2*, 625.
[31] L. Echegoyen, A. Ortiz, M. N. Chaur, A. J. Palkar in *Chemistry of Nanocarbons* (Ed.: T. Akasaka, F. Wudl, S. Nagase) Wiley, Chichester, **2010**, p. 463.
[32] K. Flavin, M. N. Chaur, L. Echegoyen, S. Giordani, *Org. Lett.* **2010**, *12*, 840.
[33] J. Bartelmess, S. Giordani, *Beilstein J. Nanotechnol.* **2014**, *5*, 1980.
[34] T. Cabioc'h, E. Thune, J. P. Rivière, S. Camelio, J. C. Girard, P. Guérin, M. Jaouen, L. Henrard, P. Lambin, *J. Appl. Phys.* **2002**, *91*, 1560.
[35] L. Joly-Pottuz, E. W. Bucholz, N. Matsumoto, S. R. Phillpot, S. B. Sinnott, N. Ohmae, J. M. Martin, *Tribol. Lett.* **2010**, *37*, 75.
[36] F.-D. Han, B. Yao, Y.-J. Bai, *J. Phys. Chem. C* **2011**, *115*, 8923.
[37] Y. Wang, F. Yan, S. W. Liu, A. Y. S. Tan, H. Song, X. W. Sun, H. Y. Yang, *J. Mater. Chem. A* **2013**, *1*, 5212.
[38] B. Xu, X. Yang, X. Wang, J. Guo, X. Liu, *J. Power Sources* **2006**, *162*, 160.
[39] N. Keller, N. I. Maksimova, V. V. Roddatis, M. Schur, G. Mestl, Y. V. Butenko, V. L. Kuznetsov, R. Schlögl, *Angew. Chem. Int. Ed.* **2002**, *41*, 1885; *Angew. Chem.* **2002**, *114*, 1962.
[40] D. Su, N. I. Maksimova, G. Mestl, V. L. Kuznetsov, V. Keller, R. Schlögl, N. Keller, *Carbon* **2007**, *45*, 2145.
[41] J. Macutkevic, R. Adomavicius, A. Krotkus, D. Seliuta, G. Valusis, S. Maksimenko, P. Kuzhir, K. Batrakov, V. Kuznetsov, S. Moseenkov, O. Shenderova, A. V. Okotrub, R. Langlet, P. Lambin, *Diamond Relat. Mater.* **2008**, *17*, 1608.
[42] D. Pech, M. Brunet, H. Durou, P. Huang, V. Mochalin, Y. Gogotsi, T.-L. Taberna, P. Simon, *Nat. Nanotechnol.* **2010**, *5*, 651.
[43] M. E. Plonska-Brzezinska, D. M. Brus, A. Molina-Ontaria, L. Echegoyen, *RSC Adv.* **2013**, *3*, 25891.
[44] M. Yang, K. Flavin, I. Kopf, G. Radics, C. H. A. Hearnden, G. J. McManus, B. Moran, A. Villalta-Cerdas, L. A. Echegoyen, S. Giordani, E. C. Lavelle, *Small* **2013**, *9*, 4194.
[45] S. Giordani, J. Bartelmess, M. Frasconi, I. Biondi, S. Cheung, M. Grossi, D. Wu, L. Echegoyen, D. F. O'Shea, *J. Mater. Chem. B* **2014**, *2*, 7459.
[46] S. Serdjukow, F. Kink, B. Steigenberger, M. Tomás-Gamasa, T. Carell, *Chem. Commun.* **2014**, *50*, 1861.
[47] J. Bartelmess, W. W. Weare, *Dyes Pigm.* **2013**, *97*, 1.
[48] L. Zhou, C. Gao, D. Zhu, W. Xu, F. F. Chen, A. Palkar, L. Echegoyen, E. S.-W. Kong, *Chem. Eur. J.* **2009**, *15*, 1389.
[49] T. Lazarides, S. Kuhri, G. Charalambidis, M. K. Panda, D. M. Guldi, A. G. Coutselos, *Inorg. Chem.* **2012**, *51*, 4193.
[50] J. Bartelmess, B. Ballesteros, G. de La Torre, D. Kiessling, S. Campidelli, M. Prato, T. Torres, D. M. Guldi, *J. Am. Chem. Soc.* **2010**, *132*, 16202.
[51] C. T. Cioffi, A. Palkar, F. Melin, A. Kumbhar, L. Echegoyen, M. Melle-Franco, F. Zerbetto, G. M. A. Rahman, C. Ehli, V. Sgobba, D. M. Guldi, M. Prato, *Chem. Eur. J.* **2009**, *15*, 4419.

Received: March 4, 2015
Published online on ■■ ■■, 0000

FULL PAPER

Know your onions: A series of bright fluorescent boron dipyrromethene (BODIPY) dyes was synthesized and characterized (see figure); single crystals of one fluorophore reveal solid-state fluorescence. Subsequently, the far-red/near-infrared-fluorescent BODIPY dye was attached to carbon nano-onions, to give a red fluorescent carbon nanomaterial.

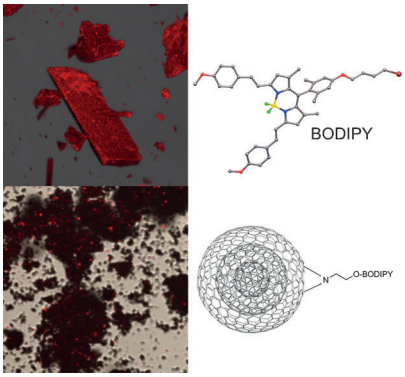

Imaging Agents

*J. Bartelmess, M. Baldrighi, V. Nardone, E. Parisini, D. Buck, L. Echegoyen, S. Giordani**

■■ – ■■

Synthesis and Characterization of Far-Red/NIR-Fluorescent BODIPY Dyes, Solid-State Fluorescence, and Application as Fluorescent Tags Attached to Carbon Nano-Onions